Journal of Non-Crystalline Solids 445–446 (2016) 34–39

Contents lists available at ScienceDirect

Journal of Non-Crystalline Solids

journal homepage: www.elsevier.com/locate/jnoncrysol

Thermal history dependence of indentation induced densification in an aluminosilicate glass

Simon Striepe [a], Joachim Deubener [a,*], Marcel Potuzak [b], Morten M. Smedskjaer [c], Anja Matthias [a]

[a] Institute of Non-Metallic Materials, Clausthal University of Technology, 38678 Clausthal-Zellerfeld, Germany
[b] Vitrex Glass, Corning, NY 14830, USA
[c] Department of Chemistry and Bioscience, Aalborg University, DK 9220 Aalborg, Denmark

ARTICLE INFO

Article history:
Received 2 March 2016
Received in revised form 21 April 2016
Accepted 30 April 2016
Available online 16 May 2016

Keywords:
Aluminosilicate glass
Fictive temperature
Vickers indentation
Thermal recovery

ABSTRACT

The mechanical properties of glasses are not only determined by their chemical composition, but also by their thermal history, i.e., fictive temperature. In this paper, we consider an alkaline earth aluminosilicate glass composition which has been annealed to exhibit a wide range of fictive temperatures (~130 K). Hardness and brittleness index have previously been shown to increase with decreasing fictive temperature, whereas the crack resistance decreases. Through quantification of the indentation depth before and after heat treatments, we show that these changes in micromechanical properties arise from an increased resistance to densification under the indenter when the glasses are annealed. We discuss these results in relation to the indentation size effect and the overall network compaction.

1. Introduction

Understanding and controlling crack initiation in brittle oxide glasses under sharp contact loading is important for developing new damage-resistant glasses. The total indentation deformation under the indenter consists of several contributions: elastic deformation, shear flow, and densification [1–5]. Elastic deformation is a reversible compression that recovers after unloading, shear flow is a volume conservative displacement of matter, and densification is a non-volume conservative irreversible compression that creates a hemispherical area of increased density beneath the imprint [6]. The relative extent of densification and shear flow depends on the chemical composition, and in turn, to the atomic packing density and Poisson's ratio ν [7]. In general, glasses with a more open network structure and smaller value of ν can be densified to a larger extent.

In addition to chemical composition, crack initiation (termed crack resistance, *CR*) is also influenced by the atmospheric conditions [8–12], thermal history [13–15], and pressure history [16,17]. For example, in a previous study [15], we reported a pronounced dependence of density and various mechanical properties on the fictive temperature T_f (i.e., thermal history) in an alkaline earth aluminosilicate glass. T_f decreases upon thermal annealing of the glass at a temperature below the initial T_f value [18]. In detail, density, Young's modulus, hardness, and brittleness increase with decreasing T_f, whereas indentation fracture toughness and *CR* decrease. It is expected that since T_f affects the atomic packing density and the elastic response of a glass, the indentation deformation mechanism should be different in glasses with different fictive temperatures.

The elastic response is difficult to measure once the indenter pyramid has been unloaded whereas the volume contributions associated with the irreversible deformation mechanisms can be quantified. This is because an indentation impression can be partially recovered by thermal annealing [1,19] which leads to a shrinkage of the imprint. This can be used to quantify the contribution of densification to the overall indentation deformation by measuring the imprint topography before and after thermal annealing. A method has been proposed by Yoshida et al. [20] with annealing for 2 h at $0.9T_g$, where T_g is the glass transition temperature (in Kelvin). This approach has been applied in various studies to characterize the indentation deformation mechanism of glasses [6,17,21–24].

To the best of our knowledge, the dependence of the contribution of densification during indentation on the fictive temperature has not previously been studied. In this work, we investigate the indentation deformation mechanism of an aluminosilicate glass with different thermal histories by performing annealing experiments and subsequent measurements of the imprint topography with 3D laser scanning microscopy. The load dependence of hardness as function of the fictive temperature is also examined as it may provide additional insights into the indentation deformation mechanism. That is, hardness decreases with increasing indentation load [25–29] and the origin of this so-called indentation size effect (ISE) has been discussed in various publications and attributed to effects such as the creation of new surface [30], friction [31], subsurface cracking [32], and presence of dislocations

* Corresponding author.
E-mail address: joachim.deubener@tu-clausthal.de (J. Deubener).

http://dx.doi.org/10.1016/j.jnoncrysol.2016.04.046
0022-3093/

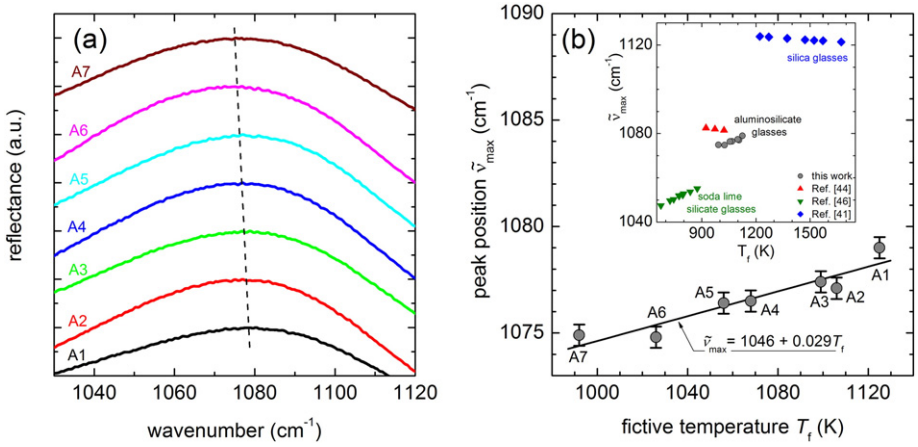

Fig. 1. (a) Infrared (IR) reflectance spectra of the glasses with varying fictive temperature. The dashed line is intended as visual guide. (b) Peak position $\tilde{\nu}_{max}$ of the IR stretching reflectance band as function of fictive temperature T_f. The line is the best linear fit through the data (regression coefficient $R^2 = 0.88$). Insert shows $\tilde{\nu}_{max}$ vs. T_f of different glass compositions. Data from Refs. [41,44,46].

[33]. The extent of ISE has been found to be composition dependent, e.g., it has been found that glasses which exhibit the largest change in density due to thermal annealing [34] or isostatic compression [35], exhibit the largest ISE. It is therefore also interesting to evaluate the thermal history dependence of ISE.

2. Experimental

The object of our study is a commercial alkaline earth aluminosilicate composition with glass transition temperature $T_g = 1055$ K [36] used for p-Si liquid crystal display substrates [37]. As described in detail elsewhere [15], glass sheets with dimensions of approximately $25 \times 25 \times 0.7$ mm^3 were annealed for various times t_a at $T_a = 973$ K (~$0.92T_g$) in order to obtain a wide range of fictive temperatures. The glasses are labeled as A1 through A7, where A1 is the as-prepared glass with the highest T_f equal to 1125 K, while A7 is the sample annealed for the longest duration with the lowest T_f equal to 992 K. In detail, the glasses were annealed for the following times t_a: 0 min (A1), 30 min (A2), 60 min (A3), 8 h (A4), 16 h (A5), 67.5 h (A6), and 305 h (A7). We note that the measured fictive temperatures obtained by varying t_a at constant T_a represent different glass structures than those which would have been obtained by long time annealing at varying T_a [18]. However, in this study, we are concerned with the trend in indentation behavior with fictive temperature, rather than the behavior at exact fictive temperature values.

Infrared (IR) reflectance spectra of the glasses were collected using a Fourier transform infrared spectrometer (Vertex 70, Bruker, Karlsruhe, Germany). For each sample, 250 spectra at wavenumbers between 1000 and 1200 cm^{-1} with a resolution of 0.5 cm^{-1} were recorded and averaged. In order to capture the bulk glass structure samples were etched in HF (20%) for 1 h before subjected to IR reflectance measurements. The thickness of the glasses after etching in HF for 1 h was 582 μm for A1 and 576 μm for A7.

Five Vickers indents were generated on the glass samples under controlled conditions (relative humidity = 40 ± 1%, $T = 298$ K) at a load of 500 mN and dwell time of 15 s (UNAT-M, Asmec). At this load, there is no formation of radial cracks. To determine the thermal history dependence of indentation deformation mechanism, we heat treat the A1–A7 samples. In the method developed by Yoshida et al. [20], the heat treatment is performed $0.9T_g$ for 2 h, as it is assumed that no structural (density) relaxation of the glass network occurs upon this heat-treatment, i.e., only relaxation of the densified volume due to the indentation occurs. Here, we perform the heat treatment at 973 K (i.e., same temperature used for initial annealing) to eliminate or minimize changes in thermal history during this heat treatment, possibly interfering with the relaxation of the indentation densified volume. Minor changes in the absolute values of T_f can, however, not be excluded but the relative differences between the samples should be unaffected. In detail, the indented specimens were heat treated at 973 K ($0.92T_g$) for various durations t_h varying between 5 and 90 min under N_2 gas flow. The heat treatments durations were varied to investigate when the relaxation of the densified volume saturates. Following each heat treatment step, the residual indentation depth was therefore measured using a 3D laser scanning microscope (VK9700, Keyence). The ratio of the actual depth (after heat treatment) to the initial indentation depth after each specific annealing (A1–A7 samples) was defined as the recovery of indentation depth (*RID*) and calculated as [38]

$$RID = \frac{d_{initial} - d_{after}}{d_{initial}}, \quad (1)$$

where $d_{initial}$ and d_{after} are the indentation depths before and after the heat treatment, respectively.

In another set of experiments, we performed Vickers indentations at different loads ranging between 30 and 1500 mN (five indents per load) to evaluate the load-dependence of hardness (indentation size effect) as function of fictive temperature. From these imprints, Vickers hardness (H_V in GPa) was calculated as [20]

$$H_V = 1.8544 \frac{P}{l^2}, \quad (2)$$

Table 1
Indentation size l at loads P ranging between 30 and 1500 mN for the seven analyzed alkaline earth aluminosilicate glasses.

P	A1	A2	A3	A4	A5	A6	A7
	l	l	l	l	l	l	l
(mN)	(μm)	(μm)	(μm)	(μm)	(μm)	(μm)	(μm)
30	2.4	2.2	2.2	2.3	2.2	2.0	2.0
50	3.2	3.1	3.3	3.3	3.3	3.0	2.9
100	4.8	4.7	4.7	4.8	4.6	4.6	4.4
200	7.0	7.2	7.0	7.1	7.0	6.7	6.6
300	8.7	8.8	8.8	8.8	8.7	8.6	8.4
400	10.2	10.2	10.3	10.4	10.1	10.0	9.9
500	11.6	11.7	11.7	11.8	11.5	11.4	11.4
750	14.3	14.6	14.7	14.5	14.3	14.1	14.2
1000	16.8	17.0	17.1	17.0	16.8	16.5	16.7
1500	21.3	21.0	21.1	20.9	20.7	20.4	20.6